View metadata, citation and similar papers at core.ac.uk

brought to you by CORE

provided by IntechOpen

We are IntechOpen, the world's leading publisher of Open Access books Built by scientists, for scientists

4,800
Open access books available

122,000
International authors and editors

135M
Downloads

Our authors are among the

154
Countries delivered to

TOP 1%
most cited scientists

12.2%
Contributors from top 500 universities

CLARIVATE ANALYTICS BOOK CITATION INDEX INDEXED

WEB OF SCIENCE™

Selection of our books indexed in the Book Citation Index in Web of Science™ Core Collection (BKCI)

Interested in publishing with us?
Contact book.department@intechopen.com

Numbers displayed above are based on latest data collected.
For more information visit www.intechopen.com

5

Kinetics and Thermodynamics of Protein Folding

Hongxing Lei[1,2] and Yong Duan[2,3]
[1]*Beijing Institute of Genomics, Chinese Academy of Sciences, Beijing*
[2]*UC Davis Genome Center and Department of Applied Science, One Shields Avenue, Davis*
[3]*College of Physics, Huazhong University of Science and Technology, Wuhan*
[1,3]*China*
[2]*USA*

1. Introduction

Proteins are the major functional elements in the living cells. Genetic information is stored in DNA. To release this information, DNA needs to be transcribed into mRNA which in turn is translated into protein. The alphabets are four bases for DNA and twenty amino acids for protein. The genetic code was revealed in 1950s with every amino acid coded by three consecutive bases. However, the amino acid sequence is only the primary structure of proteins. For proteins to be functional, the primary structure needs to fold into tertiary structure which is the optimal packing of secondary structures, namely alpha-helix and beta-sheet. In some cases, the tertiary structures of several proteins or subunits need to come together and form quaternary structure. The so-called "protein folding" problem mainly concerns the detailed physical transition process from primary structure to tertiary structure.

Protein folding mechanism consists of two major issues: kinetics and thermodynamics. Thermodynamically, the native state is the dominant and most stable state for proteins. Kinetically, however, nascent proteins take very different routes to reach the native state. Both issues have been extensively investigated by experimental as well as theoretical studies. The pioneering work by Christian Anfinsen in 1957 led to the creation and dominance of the "thermodynamic hypothesis" (also called "Anfinsen's dogma") which states that the native state is unique, stable and kinetically accessible free energy minimum(Anfinsen 1973). Under this guidance, many works have been done to pursue the illusive kinetically accessible folding pathways. One of the most famous earlier example is the "Levinthal's paradox" presented by Cyrus Levinthal in 1968, which states that the conformational space of proteins is so large that it will take forever for proteins to sample all the possible conformations before finding the global minimum(Levintha.C 1968). This essentially eliminated the possibility of global conformational search and pointed to the optimized folding pathways.

Towards this end, several well-known theories have been presented. The "framework theory" or similar "diffusion-collision theory" states that the formation of secondary structures is the first step and foundation of the global folding(Karplus and Weaver 1994). The "nucleation condensation theory", on the other hand, emphasizes the contribution from

specific global contact as the initiation point of both secondary structure formation and global folding(Fersht 1995). In contrast to the emphasis on native contacts -- global or local— in these two theories, the "hydrophobic hydration theory" states that the general repulsion between hydrophobic residues and water environment drives the spatial redistribution of polar and non-polar residues and the eventual global folding(Dill 1990). In the more recent "funnel theory", the kinetics and thermodynamics of protein folding are better illustrated as funnel-shaped where both conformational space (entropy) and energy (enthalpy) gradually decrease and numerous kinetic traps exist en route to the global folding(Bryngelson, Onuchic et al. 1995). However, the driving force for protein folding is not specified in this theory.

In order to prove or disprove any theory, experimental evidence is needed. There are several techniques developed or applied to protein folding problem. First, the structure of the investigated protein needs to be solved by X-ray crystallography or NMR (nuclear magnetic resonance). High resolution X-ray structure is preferred. However, many of the model proteins can not be crystallized, therefore only NMR structures are available. Circular dichroism (CD) is one of the classical techniques for protein folding study. The proportion of secondary structures can be reflected in CD spectrum. The change of CD spectrum under different temperature or denaturant concentration can be used to deduce melting temperature or unfolding free energy. To study the fast folding process, however, CD itself is insufficient. Fast, time-resolved techniques include ultrafast mixing, laser temperature jump and many others. Other than CD, natural or designed fluorescence probes can be used to monitor the folding process. It should be noted that the "real" folding process may not be reflected with high fidelity in these folding experiments due to the artificial folding environment. In the living cells, proteins are synthesized on ribosome one residue at a time and the final products exist in a crowded physiological condition. In the folding experiments, however, proteins stay in free artificial solution and undergo various perturbations such as denaturation. In addition, fluorescence signal of specific probes can not be simply interpreted as the global protein folding, rather it only reflects the distance between the two selected residues.

Apart from experiments, computer simulation is another approach to study protein folding mechanism. In the early days, due to the limited computing resources, protein folding simulations were performed with extremely simplified models such as lattice models and off-lattice models where each residue is represented as a bead and the movement of the residues is restricted. This gradually evolved into models with more and more realistic main chain and side chain representations including the popular all-atom models in the present era. The treatment of the solvent environment has also been evolving. The solvent was ignored in the earlier simulations (*in vacuo* simulations). Continuum models with different levels of sophistication have been developed over the years, including the most simple linear distance dependent model and the modern generalized Born (GB) models and Poisson Boltzmann (PB) models(Onufriev, Bashford et al. 2004). With the continuous growing of computing power, explicit representation of water atoms has also been used in many folding simulations.

The first ever microsecond folding simulation was performed with explicit solvent in 1998(Duan and Kollman 1998). With the help from a super computer cluster, this simulation was 100-1000 times longer than any other folding simulation at that time, thus stimulated great interest from the general public. In this simulation, the folding pathway to an intermediate state was observed. The folding rate of 4.2 μs predicted based on the simulation was highly consistent with later experimental finding of 4.3 μs. The success of

this milestone work was followed by the highly publicized folding@home project and IBM blue gene project among many other works(Zagrovic, Snow et al. 2002). It should be noted that thousands or more simulation trajectories are utilized in the folding@home project which so far can not reach the time scale for protein folding. The limitation is due to the use of idle personal desktop computers which has far less computing power than super computers. The IBM blue gene project can overcome this problem by building extremely powerful computers that can cover millisecond folding simulation. However, it has yet to make a significant progress in protein folding. In a recently published work, a specially designed super computer succeeded in the folding of two small proteins(Shaw, Maragakis et al.). Although computing power does not seem to be the greatest hurdle from now on, this success is unlikely to extend broadly in the near future. The greater challenge lies in the accuracy of simulation force fields which will be discussed later.

In this chapter, we focus on theoretical studies of protein folding by molecular dynamics simulations. The kinetics of protein folding can be studies by conventional molecular dynamics (CMD). But the insufficient sampling in current CMD simulations prevents the extraction of thermodynamic information. This has prompted the development of enhanced sampling techniques, among which the most widely adopted technique is replica exchange molecular dynamics (REMD), otherwise called parallel tempering. In the past few years, we have applied both CMD and REMD to the *ab initio* folding – meaning folding from extended polypeptide chain without any biased force towards the native contacts – of several model proteins, including villin headpiece subdomain (HP35), B domain of protein A (BdpA), albumin binding domain (ABD), and a full sequence design protein (FSD). To enhance the conformational sampling, we used an implicit solvent model GB/SA (surface area) implemented in the AMBER simulation package. The accuracy of protein folding reached sub-angstrom in most of these simulations, a significant improvement over previous simulations. Based on these high accuracy simulations, we were able to investigate the kinetics and thermodynamics of protein folding. The summary of our findings will be presented here in details. Finally, we will stress the critical role of force filed development in studying folding mechanism by simulation.

2. Kinetics and thermodynamics from *ab initio* folding simulations

2.1 Villin headpiece subdomain: Traditional analysis

Villin headpiece subdomain (HP35) is a small helical protein (35 residues) with a unique three helix architecture (Fig 1). Helix I is nearly perpendicular to the plane formed by helices II and III. The three-dimensional structure was solved earlier by an NMR experiment and more recently by a high resolution X-ray experiment(Chiu, Kubelka et al. 2005). Due to the small size and rich structural information, HP35 has attracted a lot of attention from both experimentalists and theoreticians.

In our previous works, we have conducted CMD to study the folding pathway and REMD to study the thermodynamics of HP35(Lei and Duan 2007; Lei, Wu et al. 2007). In the CMD work, we observed two intermediate states from the twenty folding trajectories (1μs each), one with the well-folded helix II/III segment (defined as the major intermediate state) and the other with the well-folded helix I/II segment (defined as the minor intermediate state). The best folded structure had C_α-RMSD of 0.39 Å and the most representative folded structure had C_α-RMSD of 1.63 Å. The productive folding always went through the major intermediate state while no productive folding was observed through the minor

intermediate state. Further examination revealed that the initiation of the folding was around the second turn between Phe17 and Pro21 rather than the hydrophobic core formed by Phe6/Phe10/Phe17. On the other hand, Gly11 was likely most accountable for the flexibility of helix I. In addition, the high occupancy of short-distance native contacts and low occupancy of long-distance native contacts pointed to the importance of local native contacts to the fast folding kinetics of HP35.

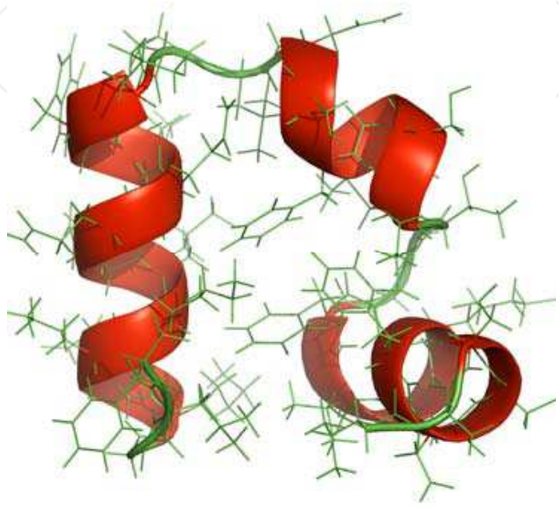

Fig. 1. Structure of villin headpiece subdomain (HP35)

In the REMD work, we conducted two sets of REMD simulations (20 replicas and 200 ns for each replica) with convergent results. The best folded structure had C_α-RMSD of 0.46 Å and the most representative folded structure had C_α-RMSD of 1.78 Å. The folding landscape of HP35 was partitioned into four thermodynamic states, namely the denatured state, native state, and the two aforementioned intermediate states. The dynamic feature of the folding landscape at selected temperatures (300 K, 340 K and 360 K) was consistent in both REMD simulations and the corresponding CMD simulations. A major free energy barrier (2.8 kcal/mol) existed between the denatured state and the major intermediate state, while a minor free energy barrier (1.3 kcal/mol) existed between the major intermediate state and the native state. In addition, a melting temperature of 339 K was predicted from the heat capacity profile, very close to the experimentally determined melting temperature of 342 K.
Because of the small size, HP35 has been considered as a classical two-state folder. This notion is supported by some earlier folding experiments. However, our simulation clearly pointed to the existence of folding intermediates. Our two-stage folding model is supported by some more recent folding experiments. In a laser temperature-jump kinetic experiment, the unfolding kinetics was fit by a bi-exponential function, with slow (5 μs) and fast (70 ns) phases. The slower phase corresponds to the overall folding/unfolding, and the fast phase was due to rapid equilibration between the native and nearby states. In a solid-state NMR study, three residues (Val9, Ala16, and Leu28) from the three helices exhibited distinct behavior during the denaturation process, and a two-step folding mechanism was proposed. In an unfolding study using fluorescence resonance energy transfer, Glasscock and co-workers demonstrated that the turn linking helices II and III remains compact under the

denaturation condition(Glasscock, Zhu et al. 2008), suggesting that the unfolding of HP35 consists of multiple steps and starts with the unfolding of helix I. In a mutagenesis experiment, Bunagan et al. showed that the second turn region plays an important role in the folding rate of HP35(Bunagan, Gao et al. 2009). A recent freeze-quenching experiment by Hu and co-workers revealed an intermediate state with native secondary structures and nonnative tertiary contacts(Hu, Havlin et al. 2009). These experiments are highly consistent with our observations in terms of both the stepwise folding and the rate-limiting step. Kubelka et al. proposed a three-state model in which the interconversion between the intermediate state and folded state is much faster than that between the intermediate state and the unfolded state(Kubelka, Henry et al. 2008). Therefore, the intermediate state lies on the folded side of the major free energy barrier, which is consistent with the separation of the unfolded state from the other states in our folding simulation. The estimation of 1.6–2.0 kcal/mol for the major free-energy barrier is also consistent with the estimation from our previous REMD simulation.

Nevertheless, controversy still exists regarding the folding mechanism of this small protein. In a recent work by Reiner et al., a folded segment with helices I/II was proposed as the intermediate state(Reiner, Henklein et al.), which corresponds to the off-pathway minor intermediate state in our work. It should be noted that different perturbations to the system, including high concentrations of denaturant, high temperatures, and site mutagenesis, have been utilized in different folding experiments. Because of the small size of HP35, the folding process may be sensitive to some of these perturbations. With the continuous development of experimental techniques that allow minimal perturbation and monitoring of the folding process at higher spatial and temporal resolution, the protein-folding mechanism will become more and more clear.

2.2 Villin headpiece subdomain: Network analysis

REMD is one of the most efficient sampling techniques for protein folding. However, due to the non-physical transitions from the exchange of conformations at different temperatures, its usage is mostly restricted to thermodynamics study. To get better understanding of the kinetics, we decided to extend the CMD simulations from the previous 1 μs to 10 μs in five selected simulation trajectories(Lei, Su et al.). Consistent with REMD, the folding free energy landscape displayed four folding states (Fig 2), the denatured state on the upper right region, the native state on the lower left region, the major intermediate state on the lower right region, and the minor intermediate state on the upper left region. The construction of the 2D landscape was based on two selected reaction coordinates, RMSD of segment A (helix I/II) and segment B (helix II/III). All five trajectories were combined together, and the population of each conformation in a small zone was converted to free energy by log transformation. From the folding landscape, we can see focused sampling in the native state, sparse sampling in the minor intermediate states, and heterogeneous sampling in the denatured state and the major intermediates state. The heavy sampling in the denatured state was likely due to the limited simulation trajectories. Ideally, thousands of trajectories are needed to reach good sampling. However, long simulations like this one are computer intensive beyond the capacity of a typical institution.

The above-described 2D landscape is only an overall display of the conformational sampling. To get more details, we performed conformational clustering based on the combined five trajectories. We here use the top ten most populated conformational clusters to describe the conformational sampling (Fig 3). The center of each conformational cluster

was used to represent the cluster. Among the top ten clusters, we can see three conformations in the native state (clusters 2, 3 and 10, colored in purple), three conformations in the major intermediate state (clusters 5, 6 and 9, colored in green), and four conformations in the denatured state (clusters 1, 4, 7 and 8, colored in blue), while the minor intermediate state did not show up due to small overall population. The overall energy (enthalpy) was not a good indication of the folding. In fact, the energy of the native state conformations was the highest and that of the denatured state conformations was the lowest. This observation did not violate the "thermodynamics hypothesis" because the conformational entropy was not included in the energy calculation. Entropy evaluation has long been a difficult subject in the field of computational biochemistry. A breakthrough will extend the application of force fields to protein structure prediction.

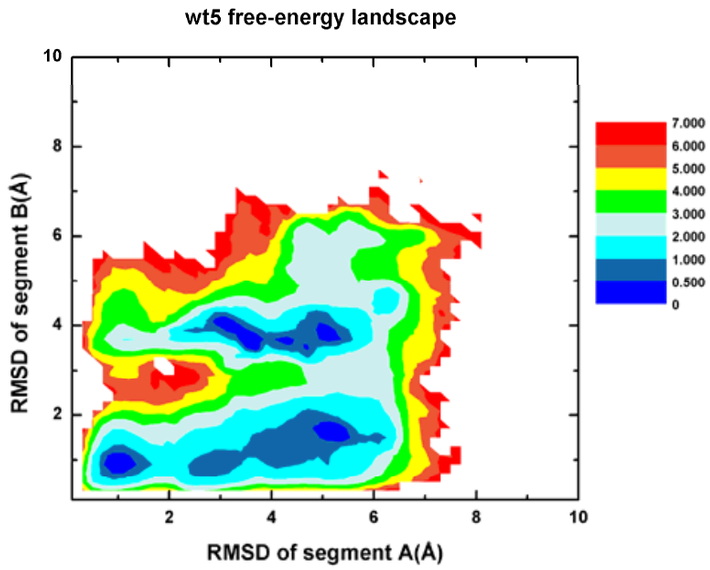

Fig. 2. Folding free energy landscape of HP35

Based on conformational clustering, we can study the kinetics and thermodynamics of protein folding using a new technique called network analysis. Traditionally, protein folding is illustrated by 1D profiles such as RMSD (global or partial), energy, solvent accessible surface area, radius of gyration and selected distances. The hyper-dimensional nature of protein folding makes none of these 1D profiles adequate to reflect the folding process. The emergence of 2D maps such as the one in Fig 2 greatly alleviate the problem by combining two independent profiles in one map. However, 2D maps are still insufficient to represent the hyper-dimensional process. Under this circumstance, several novel approaches have been applied to protein folding in recent years, including the disconnectivity graph by Karplus and network analysis pioneered by Caflisch(Krivov and Karplus 2004; Caflisch 2006).

Network analysis has gained popularity in protein folding recently(Bowman, Huang et al.; Jiang, Chen et al.). In network analysis, protein conformations are represented as nodes and the transitions among different conformations are represented as edges. Both nodes and edges can be colored based on a specified property, and analysis can be done based on the topological distribution of conformations with a specified property. In the folding network

of the combined five trajectories (Fig 4), we painted the nodes according to the state identity of the conformation and displayed the structure of the top ten populated conformations. From this network, we can see the clear separation of the denatured state from the native state and major intermediate state. The minor intermediate state was also connected to the denatured state. These findings were consistent with the observation from the 2D maps. A new finding is the mixing of the native state and major intermediate state which were clearly separated in the 2D map. The implication of this new finding is that the barrier between these two states is so small that they can easily convert to each other, which is supported by experimental evidence. This study demonstrated the power of network analysis and suggested more caution on interpreting 2D maps of protein folding.

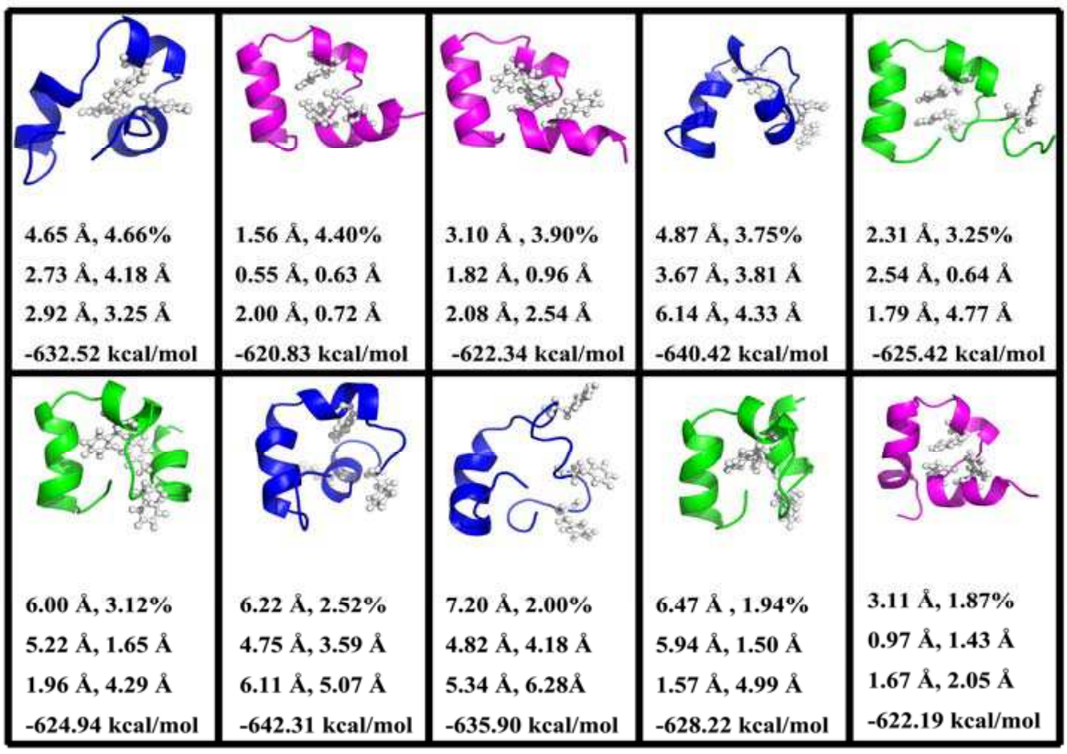

Fig. 3. Representative structures of the top ten populated clusters of HP35

The global folding network better reflect the thermodynamics of protein folding. To understand the kinetics of protein folding better, a simplified network with shortest path can be constructed (Fig 5). In this network, the shortest path connecting the denatured state, the major intermediate state and the native state was extracted from the global network. A clear flow of conformational transition from the denatured state to the major intermediate state and then to the native state was demonstrated in this network. Even the number of transitions between any neighboring conformations can be labeled on the network. In the denatured state, there were three short paths from the four top conformations to the major intermediate state, suggesting multiple folding pathways. Two conformations in the minor intermediate state were embedded in the denatured state, suggesting them as off-pathway intermediate. In the major intermediate state, the two top conformations close to the denatured state (clusters 6 and 9 in Fig 3) had wrongly folded segment A, while the top

conformation close to the native state (cluster 5 in Fig 3) had a near native structure. This information on the intra-state conformational transition is also helpful to reveal the details in the protein folding process. In the native state, the high connectivity among the conformations within the state and also with the major intermediate state suggests the relative independence of the native state and the low barrier between the native state and the major intermediate state.

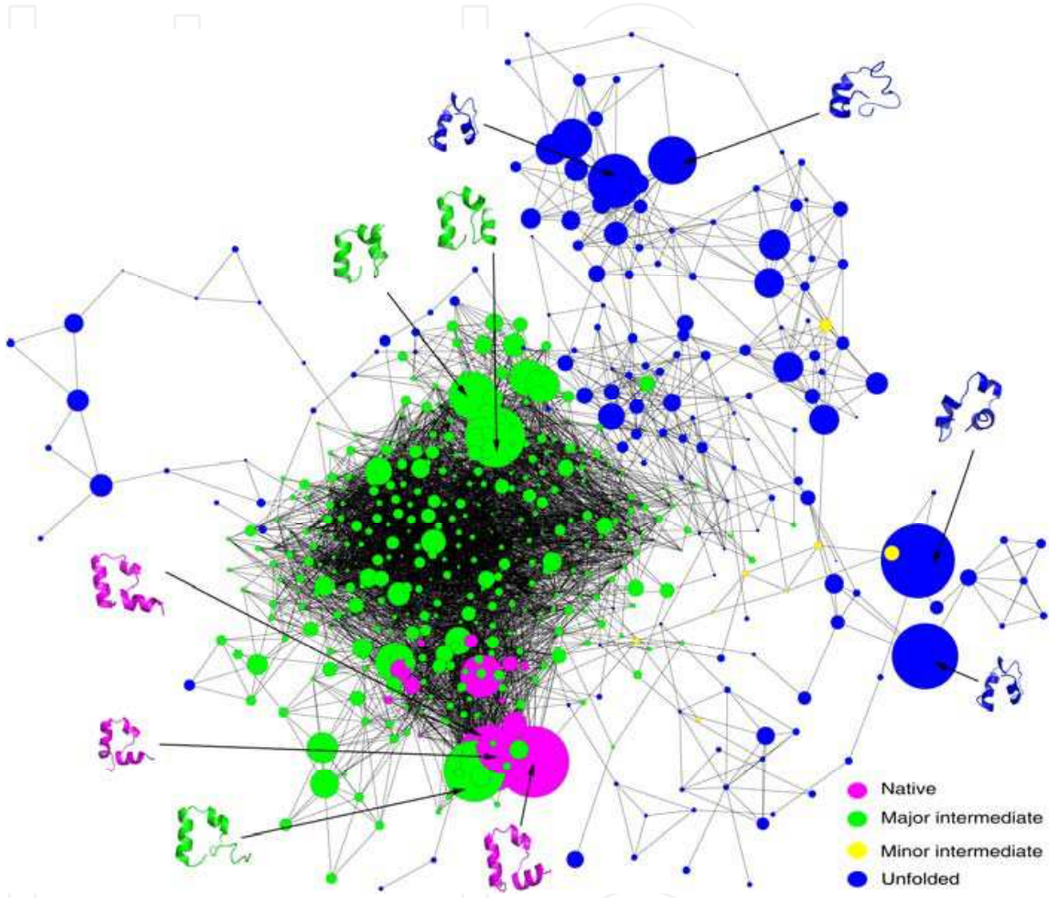

Fig. 4. Folding network of HP35

In the above two sub-sections, we have presented our study of folding mechanism for HP35 wild type. A challenging problem in this field is whether mutational effect can be reproduced in simulation. To enhance the folding rate of HP35 wild type, a mutant was designed to replace two partially buried lysine residues with non-natural neutral residues which resulted in the sub-microsecond folding. We conducted similar simulations for this HP35 mutant and compared with that of the wild type. Similar to the wild type, the mutant simulation also reached sub-angstrom accuracy(Lei, Deng et al. 2008). The folding free energy landscape also displayed similar feature with four folding states. However, some difference was also observed, especially the increased population of the native state, the decreased population of the denatured state, higher melting temperature, and the lower free energy barrier between the denatured state and the major intermediate state. These pointed to higher stability of the native state and faster folding which is consistent with the experiment. A surprising finding is the folding pathways through both intermediate states.

Therefore, the two mutated residues not only stabilized the local secondary structure (helix III), but also reshaped the folding landscape in several different ways. This kind of detailed information can not be obtained from folding experiment as yet. Thus, computer simulation will play a complimentary role in the understanding of folding mechanism in the foreseeable future.

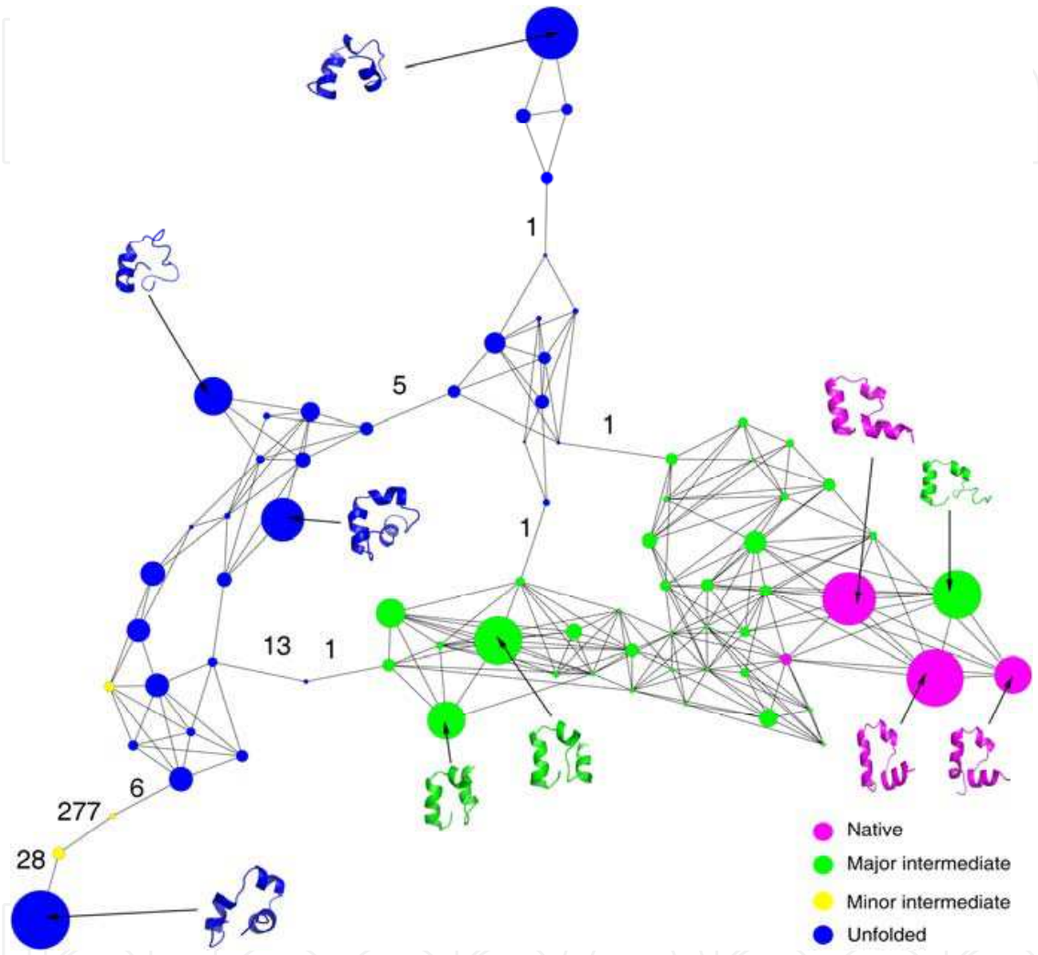

Fig. 5. A simplified folding network of HP35

2.3 Folding of three other model proteins

In addition to the folding studies of HP35 wild type and mutant, we also conducted ab initio folding on three other model proteins, namely B domain of protein A (BdpA), albumin binding domain (ABD), and a full sequence design protein (FSD). Here we will briefly describe our results. For detailed information, please refer to the original publications. BdpA is another three-helix protein with a different tertiary architecture (Fig 6). Helices II and III are relatively parallel to each other and form a plane. Helix I docks to this plane with a tilt angle relative to the other two helices. BdpA has 60 residues in the full length version and 47 residues in the truncated version (residues 10-56) where the unstructured terminal residues are trimmed off. In our simulation work, ab initio folding on both versions has been conducted.

Fig. 6. Structure of B domain of protein A (BdpA)

Successful folding was achieved in our simulation(Lei, Wu et al. 2008). The best folded structure was 0.8 Å RMSD in the CMD of truncated version and 1.3 Å in the REMD of full length version. In the CMD simulations, the folding initiated from the formation of helix III, followed by the folding of a intermediate state with well folded helix II/III segment, and completed with the docking of helix I to the helix II/III segment. The folding pathway was similar to that of HP35 except for the initiation step, where it was the formation of helix III for BdpA and formation of the second turn for HP35. In the REMD simulations, the most populated conformation was a folded conformation with 64.1% population. The melting temperature of 362 K from the heat capacity profile was also close to the experimentally derived melting temperature of 346 K. From the calculated potential of mean force, the native state was 0.8 kcal/mol favored over the denatured state, and the free energy barrier from the denatured state to the native state was 3.7 kcal/mol. These findings were in qualitative agreement with folding experiments of BdpA. In addition, we tested the structure prediction performance based on AMBER potential energy and DFIRE statistical energy. Both gave similar performance with most predicted structures near 3.0-3.5 Å RMSD, while the structure with the lowest AMBER potential energy was only 2.0 Å RMSD.

Albumin binding domain (ABD) is yet another three helix protein with different topological feature from both HP35 and BdpA (Fig 7). Helices I and III are relatively long and parallel with each other, while the shorter helix II serves as linker. NMR studies revealed high uncertainty in the first loop and dynamics around helix II. The experimentally determined folding rate for wild type ABD is 6 μs. Enhanced folding rate was achieved in two mutants (2.5 μs for K5I and 1.0 μs for K5I/K39V).

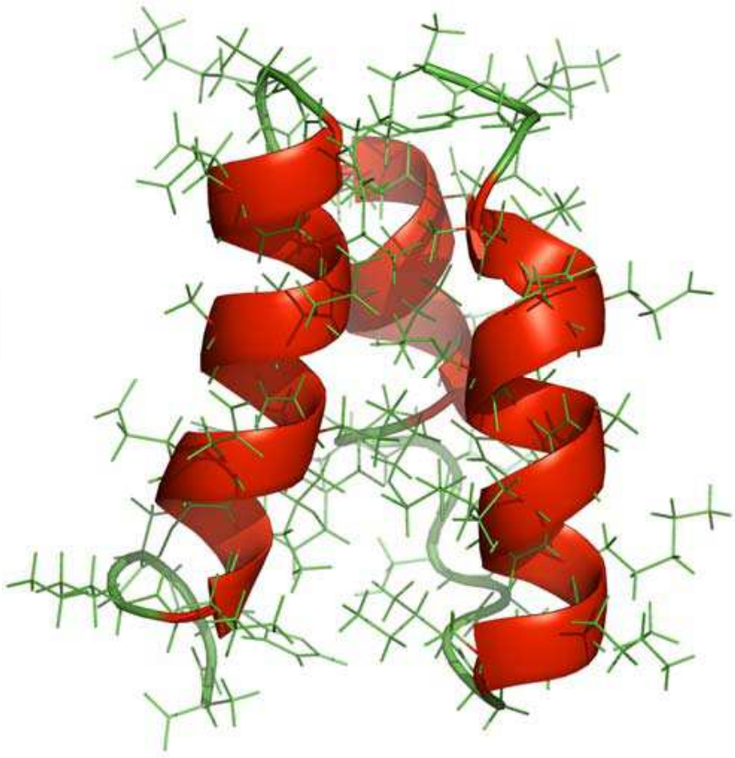

Fig. 7. Structure of albumin binding domain (ABD)

We conducted 20 CMD simulations (400 ns each) for each of the above mentioned three ABD variants. Although the size of ABD is comparable to the truncated BdpA (both 47 residues), no successful folding of ABD was reported prior to our study. In our simulations, the best folded structure reached 2.0 Å RMSD, indicating the first ever successful folding of ABD(Lei and Duan 2007). The folding started from the formation of helix I, followed by the formation of the other two helices, and completed by the optimal packing of the three helices. Although two hydrophobic cores exist in the middle, their formation was late in the simulation, suggesting that they are not the driving force of the global folding. Examination of conformational sampling revealed that the folded conformation was the most populated and significant formation of helices also appeared in other populated conformations. Compared to HP35 and BdpA, the accuracy of folding was lower for ABD. This was likely coming from several sources. First, ABD is highly dynamic according to NMR experiments which makes it difficult to choose a reference structure to determine folding accuracy. Second, the trajectory length for ABD (400 ns) was significantly shorter than that of HP35 and BdpA (both 1 μs). Third and likely most importantly, some features in ABD can not be modeled well in the current simulation force fields. The hydrophobic core in ABD may play important role in the folding mechanism, while it may play minor role in the folding of HP35 and BdpA. Therefore, inaccurate modeling of hydrophobic interaction will lead to less accurate folding of ABD than that of HP35 and BdpA. In addition, helix boundaries were slightly shifted in the simulation compared with the NMR structure, which may be partially due to the inaccurate parameterization of certain amino acids such as Valine.

The three model proteins described above are all helical proteins. A more challenging task is to fold proteins with both alpha-helix and beta-sheet secondary structures. Full sequence

design protein (FSD) is a designed 28- residue α/β protein. Our previous attempts on the ab initio folding of FSD were unsuccessful with the same simulation force field (AMBER FF03) used in the successful folding of the three helical proteins. Therefore, we decided to re-parameterize the force field under the same solvation scheme (GB/SA) for a better balance of the two major secondary structures.

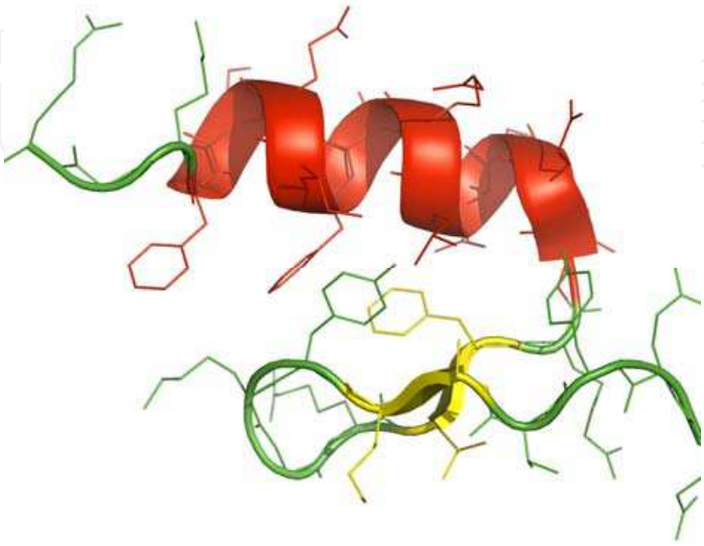

Fig. 8. Structure of a full sequence design protein (FSD)

Using the newly developed force field, we conducted ab initio folding of FSD with both CMD and REMD(Lei, Wang et al. 2009). High accuracy folding was achieved in terms of both the best folded structure (0.8 Å RMSD) and the population of the folded conformation (64.2%). High diversity was observed in the sampled denatured conformations, including a long helix, a helix hairpin and a long beta-hairpin, indicating good balance of the two major secondary structures. The folding of FSD followed two distinctive pathways. The major pathway began with the formation of the helix, while the minor pathway started with the formation of the beta-hairpin. More specifically, the initiation of the helix started from the C-terminal and propagated to the N-terminal. The free energy profiles showed different stability for the two structural elements. For the helix segment, the native helical structure had significantly lower free energy than other conformations. For the hairpin segment, however, 2-3 non-native conformations existed with similar free energy, which led to several local traps on the free energy landscape. Kinetically, the free energy barrier was similar for the folding of both segments (2-3 kcal/mol), but it was a single barrier for the helix and multiple barriers for the hairpin. The melting temperature extracted from the heat capacity profile was 360 K. However, this temperature merely reflected the melting of the helix (~50% helicity at 360 K), while the population of globally folded conformation was close to 0% at 360 K. Therefore, caution should be taken when interpreting the "melting temperature" extracted from the heat capacity profile.

3. Kinetics and thermodynamics from unfolding simulations

Ideally, protein folding mechanism should be studied by ab initio folding. However, due to the limited access of super computers by most research groups, ab initio folding simulations

are limited to very few small model proteins such as listed in Section 2. For most other proteins, an alternative approach is unfolding simulation where the native starting structures gradually unfold under the high temperature. A major assumption with this approach is that folding pathway is the reverse of unfolding pathway. To validate this approach, we conducted unfolding simulations on HP35, BdpA and FSD and compared the unfolding pathways with the folding pathways from ab initio simulations. Here we mainly use the unfolding of HP35 as an example.

We conducted ten unfolding simulations of HP35 at 350 K (100 ns each) and used the average properties from these simulations to describe the unfolding process. One of the main findings from the ab initio folding simulations was the major intermediate state with well-folded helix II/III segment. Thus, we first examined the unfolding of the two structural segments (Fig 9). We can clearly see the faster unfolding of the helix I/II segment which reached complete unfolding before 20 ns. On the other hand, the unfolding of helix II/III segment was much slower and was still fluctuating after unfolding. The slower unfolding and higher stability of helix II/III segment suggest that it folds earlier than helix I/II segment, which is consistent with the finding from ab initio folding.

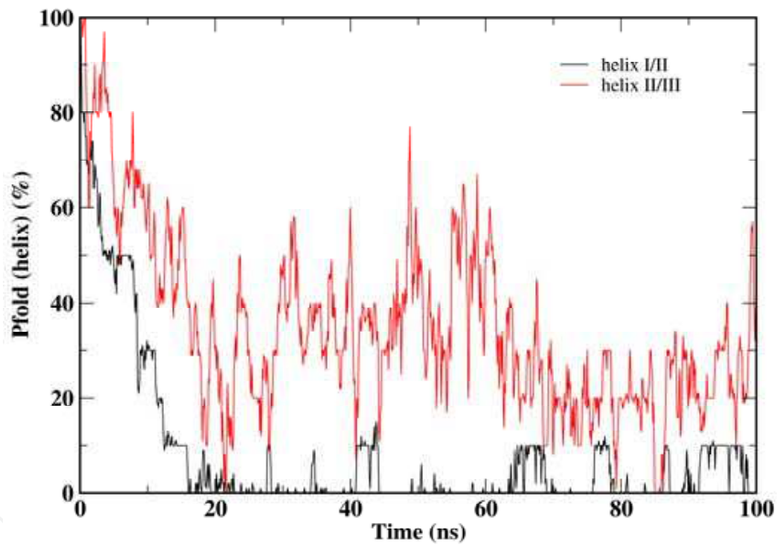

Fig. 9. Unfolding of the two segments of HP35

Second, we examined the unfolding of the three individual helices using a simple helicity measurement (Fig 10). The three helices showed distinctive unfolding features. Helix I was the fastest to unfold and the least stable one, down to 50% within 10 ns and towards 25% near 100 ns. On the other hand, helix III was the slowest to unfold and the most stable one, fluctuating between 70% and 85% during the whole simulation time. This suggests that helix III is the first to fold and helix I is the last to fold, which is also consistent with the ab initio folding simulation.

Further evaluation of the unfolding can be performed at the residue level. We calculated the root mean square fluctuation (RMSF) for each residue during the entire unfolding process (Fig 11). Overall, the two terminal regions displayed highest fluctuation and the second half of the protein was significantly more stable than the first half. Heterogeneity was observed

within the helices. Within helix I (residues 3-9), the middle residues 6 and 5 had the lowest fluctuation. Within helix II (residues 14-19), the C-terminal residues 17-19 had the lowest fluctuation. Within helix III (residues 22-31), most residues had the low fluctuation especially residues 24-30. Another interesting observation is the low fluctuation of residue 20 at the second turn. All these observations were consistent with the folding mechanism from the ab initio folding simulations.

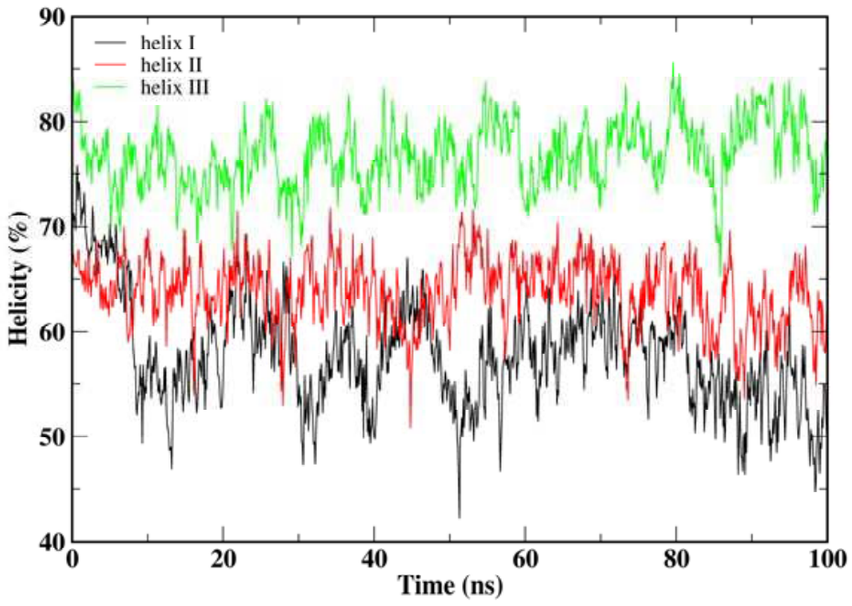

Fig. 10. Unfolding of the three helices of HP35

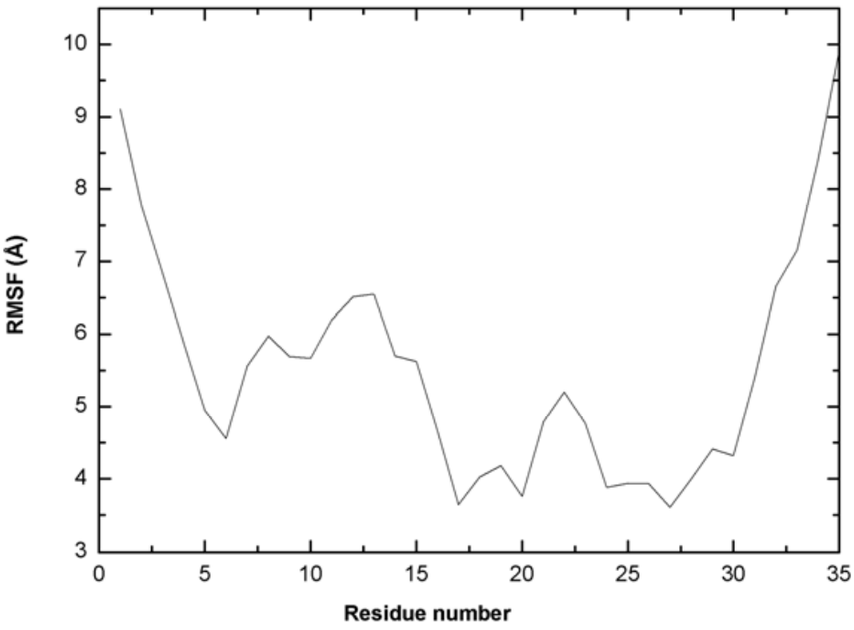

Fig. 11. Dynamic feature of each residue in the unfolding of HP35

A more intuitive way to visualize the folding pathways is by constructing the folding landscape. We divided the 100 ns unfolding time into five time frames and constructed folding landscape during each time frame (the first and last time frames shown in Fig 12). During the first time frame (0-20 ns), the native state was the most dominant one, while unfolding to the major intermediate state and denatured state was also observed. During the last time frame (80-100 ns), the denatured state became the most dominant one, while the major intermediate state was observed but the native state and the minor intermediate state were almost undetectable. The reverse of this observed process was exactly what we observed in the ab initio folding of HP35.

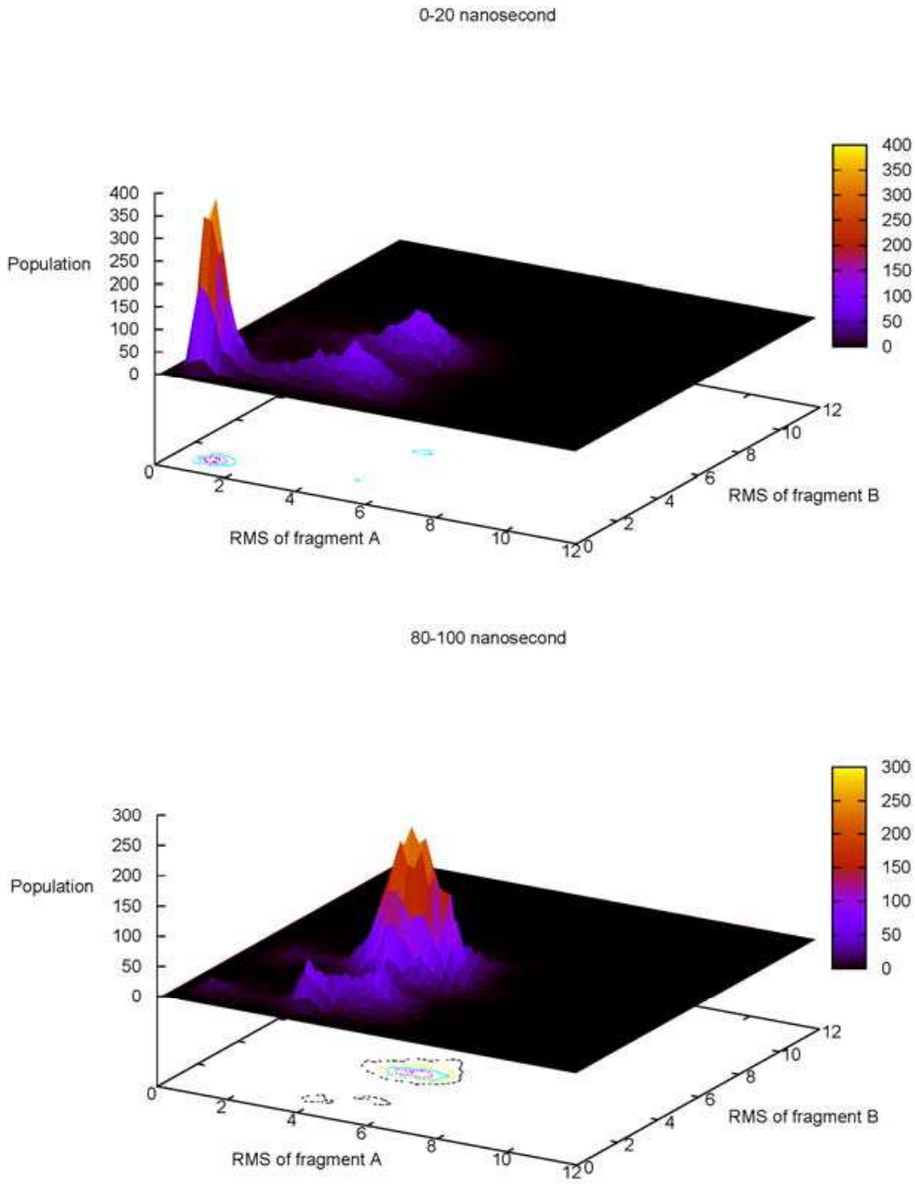

Fig. 12. Shifting of structural ensembles during the unfolding of HP35

In addition to the unfolding of HP35, we also conducted unfolding simulations on BdpA and FSD, all with ten trajectories of 100 ns simulations at 350 K. The unfolding mechanism from these two sets of simulations was also consistent with the folding mechanism from previously described ab initio folding simulations. In summary, our comparison between unfolding and ab initio folding suggests that unfolding is a valuable approach to study folding mechanism when ab initio folding is unfeasible. However, our comparison was based on three small model proteins, whether this conclusion can be extended to other proteins remains to be a question for future investigation.

4. Simulation force field development

At this point, we should stress the importance of force field in protein folding simulation. Under appropriate protocol, a simulation is as good as the underlying force field is. Currently, the main stream force fields, namely AMBER, CHARMM, GROMOS and OPLS, are all point charge models(Duan, Wu et al. 2003). Under this philosophy, a partial charge is assigned to every atom of a specific amino acid with the overall charge reflecting the charge nature of the amino acid (+1, -1 or 0). In some schemes, the main chain atoms (N, H, CA, C and O) are restricted to have the same set of partial charges for every amino acid, while this restriction was not applied in some other schemes. The partial charges can be derived from fitting to the electrostatic potential calculated by quantum mechanics, or can be assigned by chemical intuition. Another major parameterization of force field is the torsion angles, both main chain and side chain, which is usually fitted to reflect the potential energy surface of amino acid analogs especially Alanine dipeptide calculated by quantum mechanics. The major advantage of the current generation force field is the speed. However, as longer and longer simulations being conducted, more and more problems have been revealed regarding the accuracy of these force fields, including significant bias towards a specific secondary structure (alpha-helix or beta-sheet). In light of these problems, the concept of polarizable force field has emerged. The major philosophical difference from point charge models is the dynamics in charge distribution. Polarizable force fields are being developed and will likely become the next generation force field soon.

5. Conclusion

Computer simulation is a powerful tool to study the kinetics and thermodynamics of protein folding. Here we summarized our study of folding mechanism on four model proteins by CMD an REMD. We have reached sub-angstrom folding on HP35, BdpA and FSD and 2.0 Å RMSD folding on ABD. From the high quality folding simulations, we extracted a plethora of information regarding the folding mechanism, including folding pathways, folding states, free energy barriers, melting temperature and folding landscape. We have also applied network analysis to the study of folding mechanism and revealed new information about the folding of HP35. In addition, the high consistency between unfolding simulations and *ab initio* folding simulations suggest that unfolding simulations can be used as an alternative.

6. Acknowledgement

This work was supported by research grants from NIH (Grants GM79383 and GM67168 to YD), NSFC (Grant 30870474 to HL) and SRF for ROCS, SEM (to HL). Usage of AMBER and Pymol, GRACE, VMD, Matlab and Rasmol graphics packages are gratefully acknowledged.

7. References

Anfinsen, C. B. (1973). "Principles that govern the folding of protein chains." *Science* 181(96): 223-30.

Bowman, G. R., X. Huang, et al. (2010). "Network models for molecular kinetics and their initial applications to human health." *Cell Res* 20(6): 622-30.

Bryngelson, J. D., J. N. Onuchic, et al. (1995). "Funnels, Pathways, and the Energy Landscape of Protein-Folding - a Synthesis." *Proteins-Structure Function and Genetics* 21(3): 167-195.

Bunagan, M. R., J. Gao, et al. (2009). "Probing the folding transition state structure of the villin headpiece subdomain via side chain and backbone mutagenesis." *J Am Chem Soc* 131(21): 7470-6.

Caflisch, A. (2006). "Network and graph analyses of folding free energy surfaces." Current *Opinion in Structural Biology* 16(1): 71-78.

Chiu, T. K., J. Kubelka, et al. (2005). "High-resolution x-ray crystal structures of the villin headpiece subdomain, an ultrafast folding protein." *Proc Natl Acad Sci U S A* 102(21): 7517-22.

Dill, K. A. (1990). "Dominant forces in protein folding." *Biochemistry* 29(31): 7133-55.

Duan, Y. and P. A. Kollman (1998). "Pathways to a protein folding intermediate observed in a 1-microsecond simulation in aqueous solution." *Science* 282(5389): 740-4.

Duan, Y., C. Wu, et al. (2003). "A point-charge force field for molecular mechanics simulations of proteins based on condensed-phase quantum mechanical calculations." *J Comp Chem* 24(16): 1999-2012.

Fersht, A. R. (1995). "Optimization of rates of protein folding: the nucleation-condensation mechanism and its implications." *Proc Natl Acad Sci U S A* 92(24): 10869-73.

Glasscock, J. M., Y. Zhu, et al. (2008). "Using an amino acid fluorescence resonance energy transfer pair to probe protein unfolding: application to the villin headpiece subdomain and the LysM domain." *Biochemistry* 47(42): 11070-6.

Hu, K. N., R. H. Havlin, et al. (2009). "Quantitative determination of site-specific conformational distributions in an unfolded protein by solid-state nuclear magnetic resonance." *J Mol Biol* 392(4): 1055-73.

Jiang, X., C. Chen, et al. (2010). "Improvements of network approach for analysis of the folding free-energy surface of peptides and proteins." *J Comput Chem* 31(13): 2502-9.

Karplus, M. and D. L. Weaver (1994). "Protein folding dynamics: the diffusion-collision model and experimental data." *Protein Sci* 3(4): 650-68.

Krivov, S. V. and M. Karplus (2004). "Hidden complexity of free energy surfaces for peptide (protein) folding." *Proceedings of the National Academy of Sciences of the United States of America* 101(41): 14766-14770.

Kubelka, J., E. R. Henry, et al. (2008). "Chemical, physical, and theoretical kinetics of an ultrafast folding protein." *Proc Natl Acad Sci U S A* 105(48): 18655-62.

Lei, H., X. Deng, et al. (2008). "The fast-folding HP35 double mutant has a substantially reduced primary folding free energy barrier." *J Chem Phys* 129(15): 155104.

Lei, H. and Y. Duan (2007). "Ab initio folding of albumin binding domain from all-atom molecular dynamics simulation." *J Phys Chem* B 111(19): 5458-63.

Lei, H. and Y. Duan (2007). "Two-stage folding of HP-35 from Ab initio simulations." *J Mol Biol* 370(1): 196-206.

Lei, H., Y. Su, et al. (2010). "Folding network of villin headpiece subdomain." *Biophys J* 99(10): 3374-84.

Lei, H., C. Wu, et al. (2007). "Folding free-energy landscape of villin headpiece subdomain from molecular dynamics simulations." *Proc Natl Acad Sci U S A* 104(12): 4925-30.

Lei, H. X., Z. X. Wang, et al. (2009). "Dual folding pathways of an alpha/beta protein from all-atom ab initio folding simulations." *Journal of Chemical Physics* 131(16): -.

Lei, H. X., C. Wu, et al. (2008). "Folding processes of the B domain of protein A to the native state observed in all-atom ab initio folding simulations." *Journal of Chemical Physics* 128(23): -.

Levintha.C (1968). "Are There Pathways for Protein Folding." *Journal De Chimie Physique Et De Physico-Chimie Biologique* 65(1): 44-45.

Onufriev, A., D. Bashford, et al. (2004). "Exploring protein native states and large-scale conformational changes with a modified generalized born model." *Proteins* 55(2): 383-394.

Reiner, A., P. Henklein, et al. (2010). "An unlocking/relocking barrier in conformational fluctuations of villin headpiece subdomain." *Proc Natl Acad Sci U S A* 107(11): 4955-60.

Shaw, D. E., P. Maragakis, et al. (2010). "Atomic-level characterization of the structural dynamics of proteins." *Science* 330(6002): 341-6.

Zagrovic, B., C. D. Snow, et al. (2002). "Simulation of folding of a small alpha-helical protein in atomistic detail using worldwide-distributed computing." *J Mol Biol* 323(5): 927-37.

IntechOpen

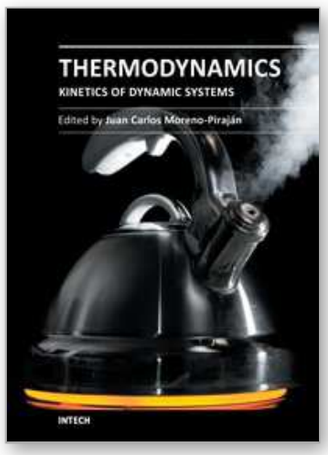

Thermodynamics - Kinetics of Dynamic Systems
Edited by Dr. Juan Carlos Moreno PirajÃ¡n

ISBN 978-953-307-627-0
Hard cover, 402 pages
Publisher InTech
Published online 22, September, 2011
Published in print edition September, 2011

Thermodynamics is one of the most exciting branches of physical chemistry which has greatly contributed to the modern science. Being concentrated on a wide range of applications of thermodynamics, this book gathers a series of contributions by the finest scientists in the world, gathered in an orderly manner. It can be used in post-graduate courses for students and as a reference book, as it is written in a language pleasing to the reader. It can also serve as a reference material for researchers to whom the thermodynamics is one of the area of interest.

How to reference
In order to correctly reference this scholarly work, feel free to copy and paste the following:

Hongxing Lei and Yong Duan (2011). Kinetics and Thermodynamics of Protein Folding, Thermodynamics - Kinetics of Dynamic Systems, Dr. Juan Carlos Moreno PirajÃ¡n (Ed.), ISBN: 978-953-307-627-0, InTech, Available from: http://www.intechopen.com/books/thermodynamics-kinetics-of-dynamic-systems/kinetics-and-thermodynamics-of-protein-folding

INTECH
open science | open minds

InTech Europe
University Campus STeP Ri
Slavka Krautzeka 83/A
51000 Rijeka, Croatia
Phone: +385 (51) 770 447
Fax: +385 (51) 686 166
www.intechopen.com

InTech China
Unit 405, Office Block, Hotel Equatorial Shanghai
No.65, Yan An Road (West), Shanghai, 200040, China
中国上海市延安西路65号上海国际贵都大饭店办公楼405单元
Phone: +86-21-62489820
Fax: +86-21-62489821

© 2011 The Author(s). Licensee IntechOpen. This chapter is distributed under the terms of the Creative Commons Attribution-NonCommercial-ShareAlike-3.0 License, which permits use, distribution and reproduction for non-commercial purposes, provided the original is properly cited and derivative works building on this content are distributed under the same license.

IntechOpen

IntechOpen